Magnetic structure of $GdCo_2Ge_2$

W. Good, J. Kim, A. I. Goldman,* D. Wermeille, P. C. Canfield, and C. Cunningham
Ames Laboratory U.S.D.O.E. and Department of Physics and Astronomy, Iowa State University, Ames, Iowa 50011, USA

Z. Islam, J. C. Lang, and G. Srajer
Advanced Photon Source, Argonne National Laboratory, Argonne, Illinois 60439, USA

I. R. Fisher
Laboratory for Advanced Materials and Department of Applied Physics, Stanford University, Stanford, California 94305-4090, USA
(Received 7 February 2005; published 29 June 2005)

Resonant and nonresonant magnetic x-ray scattering studies of $GdCo_2Ge_2$ were performed to determine its magnetic structure at low temperature. This compound orders in an incommensurate antiferromagnetic (AF) structure characterized by a propagation wave vector $\tau=(0\ 0\ \tau_z)$. The value of τ_z is temperature dependent and approaches 0.930 reciprocal lattice units well below $T_N=33.25$ K. A peak corresponding to $3\tau_z$ was also observed, indicating either a squaring up of the magnetic structure or the presence of a noncollinear amplitude modulated structure below T_N. Fitting the angular dependence of the magnetic scattering integrated intensities to the relevant resonant and nonresonant scattering cross sections revealed that the moment direction lies primarily in the tetragonal basal plane. Scattering measurements at the Co *K*- edge failed to detect any resonant signal, consistent with the absence of a magnetic moment on the Co sites.

DOI: 10.1103/PhysRevB.71.224427 PACS number(s): 75.25.+z, 75.50.Ee

I. INTRODUCTION

The interplay of long-range exchange interactions and anisotropy has been at the focal point of research in rare-earth magnetism for decades. For most of the rare-earth elements, with contributions from orbital moments, single-ion interactions due to crystal electric field (CEF) effects dominate the anisotropy of the magnetic ground state. Theoretical approaches incorporating these two effects have been quite successful in elucidating magnetically ordered states, such as commensurate and incommensurate equal moment (EM) and amplitude-modulated (AM) collinear structures of numerous rare-earth intermetallic compounds. However, the anisotropy due solely to anisotropic exchange interactions, which has its origin in the underlying electronic bands, are difficult to study when competing CEF effects are present. Recent theoretical studies suggest the formation of noncollinear amplitude modulated (NCAM) structures[1] due to such anisotropic exchange interactions even when CEF effects and higher-order interactions are absent. Gadolinium (Gd) compounds are ideal for studying these unusual magnetic ground states (since for this rare-earth ion, $L=0$ and CEF effects are absent) and for developing a deeper understanding of the role of electronic band filling on long-range order and anisotropy via exchange interactions.

The Gd member of the rare-earth cobalt germanide family (RCo_2Ge_2, where R=heavy rare earth) crystallizes in the body-centered tetragonal $ThCr_2Si_2$-type structure (space group $I4/mmm$),[2] and is of particular interest. Several of the compounds in the RCo_2Ge_2 family exhibit a transformation from an incommensurate modulated antiferromagnetic state below T_N to a collinear commensurate antiferromagnetic structure below a second transition temperature $T_T<T_N$. For $TbCo_2Ge_2$,[3,4] $DyCo_2Ge_2$, and $HoCo_2Ge_2$ (Ref. 5) reinvestigations of the magnetic structure revealed that the incommensurate wave vector in the temperature range $T_T<T<T_N$ is of the form $(0\ 0\ \tau_z)$ with τ_z ranging between 0.92 and 0.94. Below T_T, there is an abrupt change in the wave vector, jumping to the commensurate value of 1.0. In all three compounds, the magnetic moment direction is essentially along the unique c axis of the tetragonal structure for both the low-temperature commensurate and higher-temperature incommensurate phases. For $DyCo_2Ge_2$ there appears to be a slight canting away from the c axis in the low-temperature commensurate structure.[5] For $ErCo_2Ge_2$ the commensurate antiferromagnetic structure is characterized by a wave vector (001) and magnetic moment direction in the basal plane.[6]

The RCo_2Ge_2 compounds are isostructural to the RNi_2Ge_2 compounds where a robust Fermi-surface nesting is responsible for incommensurate magnetic structures,[7,8] indicating a critical role played by the underlying electronic structures in mediating exchange interactions. Recent photoemission work[9] showed that rigid-band shifts in the Ni germanides are valid and, given the close structural relationship, a similar nesting behavior may be expected in the RCo_2Ge_2 compounds as well. According to susceptibility measurements, $GdCo_2Ge_2$ exhibits only one antiferromagnetic transition unlike the $GdNi_2Ge_2$ compound in which two or more transitions are observed, indicating that higher-order interactions are important in the latter material. Thus the absence of additional low-T transitions makes $GdCo_2Ge_2$ a better candidate for the study of possible NCAM phases. Furthermore, electronic generalized susceptibility calculations for the Ni germanides showed that the nesting feature is tunable via band filling, which can be realized by alloying such as $Gd(Ni_{1-x}Co_x)_2Ge_2$ with no significant structural perturbations, providing a knob to vary the fundamental nature of the magnetic ground state.

It is clearly of interest to investigate compounds where R=Gd. All of the known $Gd(TM)_2X_2$ (TM=transition-metal

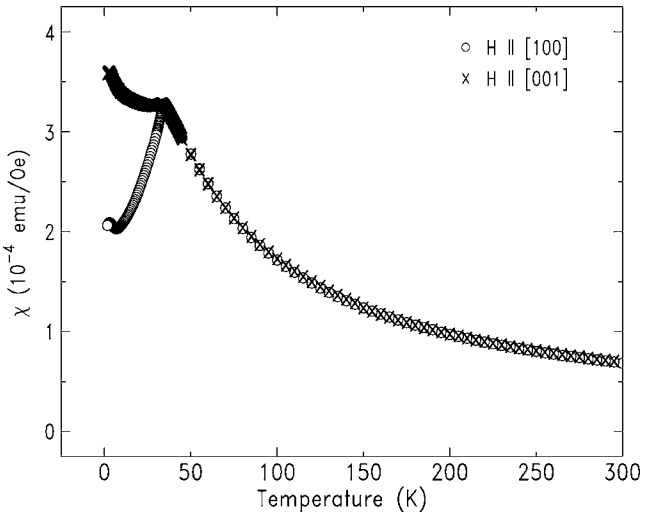

FIG. 1. SQUID susceptibility measurements with a field of $H=1$ kOe applied parallel to the c axis [001] or perpendicular to the c axis [100]. The peak in the susceptibility is at approximately 33 K.

element, X=Ge or Si) order antiferromagnetically.[10,11] Few of the magnetic structures are known in detail, however, since neutron diffraction measurements are hampered by the large absorption cross-section for naturally occurring Gd. X-ray resonant magnetic scattering (XRMS) provides an alternative to neutron measurements in these cases.[12,13] In this work, we focus on elucidating the magnetically ordered state of $GdCo_2Ge_2$ and lay the foundation for future studies of electronic tuning of magnetically ordered phases.

II. EXPERIMENTAL PROCEDURES

For our XRMS studies of magnetic ordering in $GdCo_2Ge_2$, single crystals were grown at the Ames Laboratory using a high-temperature flux growth technique.[14,15] The crystals form as platelets with the unique c axis perpendicular to the surface. The specimen with the smoothest surface, without visible flux inclusions, was chosen for the x-ray experiment and was characterized on a four circle diffractometer using a rotating anode (Mo) x-ray source. The sample mosaic was measured to be 0.012 deg at the (0 0 8) reflection. Susceptibility measurements performed at Ames Laboratory using a superconducting quantum interference device (SQUID) magnetometer exhibit a peak at approximately T_N =33 K as seen in Fig. 1. From Fig. 1, we see that the susceptibility measured with the field perpendicular to c decreases below T_N. This behavior indicates that the moments likely lie close to the tetragonal basal plane, rather than along the c axis.

Initial XRMS studies were performed on the Sector 1 bending magnet beam line[16] at the Advanced Photon Source, Argonnel, IL (APS) with the incident energy of x rays tuned to the Gd L_{III} edge (E=7.241 KeV). The bulk of the XRMS measurements were carried out on the 6-ID undulator line in the Midwest Universities Collaborative Access Team (MUCAT) Sector at the APS. A liquid nitrogen cooled, double crystal Si(111) monochromator, and a bent mirror were used to select the incident photon energy, focus the beam, and suppress higher-order harmonics. The sample was mounted on a copper rod on the cold finger of a closed cycle displex refrigerator. The sample, oriented so that the scattering plane of the experiment was coincident with the (H0L) zone, was encapsulated in a Be dome with a He exchange gas to enhance thermal transfer.

The resonant scattering measurements were carried out at the Gd L_{III} absorption edge with the incident radiation linearly polarized perpendicular to the scattering plane (σ polarized). In this geometry, only the component of the magnetic moment that is in the scattering plane (the H0L plane in this case) contributes to the resonant scattering arising from electric dipole transitions from the $2p$ to $5d$ states.[13] Furthermore, the linear polarization of the resonant scattered radiation is rotated into the scattering plane (π polarization).

A pyrolytic graphite analyzer PG (0 0 6) was used as a polarization analyzer, set to reduce the background from Thomson charge scattering. In contrast to dipole-resonant magnet scattering, charge scattering does not change the polarization of the incident beam (σ-σ scattering) For E =7.243 KeV the scattering angle for the analyzer is approximately 100 deg and so the $\sigma \rightarrow \sigma$ charge scattering is reduced by $\sim$97% while the $\sigma \rightarrow \pi$ resonant scattering is passed with little loss. This polarization selection effectively enhances the magnetic peak intensity relative to the charge background.

III. RESULTS

Based on the results from other compounds in the RCo_2Ge_2 family, a search was carried out for a modulation wave vector of the form (0 0 τ_z) with τ_z between 0.7 and 1.0. In the initial measurements on 1BM (XOR Sector), magnetic superstructure peaks characterized by (0 0 0.93) were observed. A count rate of approximately 8000 counts/s was measured for the (0 0 5.093) magnetic peak, using a Ge solid-state detector. No third harmonic of the fundamental satellite was observed above the background.

The remainder of the data presented here were collected using the MUCAT undulator beam line which offers greater sensitivity due to higher photon-flux density. Magnetic peaks were found at reciprocal space positions corresponding to (0 0 $L\pm\tau_z$), where L is an even integer as shown in Fig. 2. The magnetic peaks decrease in intensity and, finally, disappear close to the transition temperature determined by the the susceptibility measurements ($T_N \approx 33$ K).

The magnetic wave vector (τ_z) was found to be temperature dependent with a value approaching τ_z=0.930 reciprocal lattice units (rlu) at T=6 K, the base temperature of this measurement. Figure 3 displays the temperature dependence of the wave vector as determined by fitting both the (0 0 8$-\tau_z$) and (0 0 8$+\tau_z$) satellite peaks to obtain their positions relative to the (0 0 8) charge peak over the entire temperature range. The continuous change in the wave vector with temperature is indicative of an incommensurate antiferromagnetic structure. Interestingly, the magnetic wave vector increases as temperature is increased to reach a maximum of

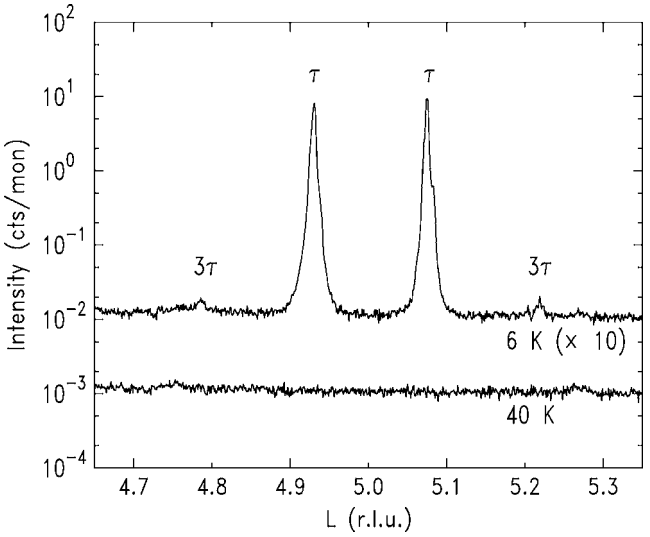

FIG. 2. Longitudinal scans across the (0 0 L) reflections at 6 and 40 K taken at the Gd L_{III} edge. The 6 K data are offset relative to the 40 K data.

0.933 rlu at $T=25$ K and then decreases as the temperature approaches T_N. While such a nonmonotonic behavior of the magnetic wave vector is often observed close to T_N, it is not well-understood at this time. Possible explanations include subtle changes in the electronic structure close to T_N which are now revealed by the high-reciprocal space resolution available to x-ray measurements.

In order to confirm that the magnetic peaks are associated with the resonant scattering process, energy scans through the Gd L_{III} edge at the (008) charge peak and (0 0 $8-\tau_z$) magnetic satellite were performed and are shown in Fig. 4. The absorption edge, defined by the maximum slope in absorption, is shown in the figure as the dashed vertical line. The observation of a resonant peak in the scattering at the magnetic satellite position, just above the Gd L_{III} edge, confirms that the enhancement arises from dipole resonant scattering.

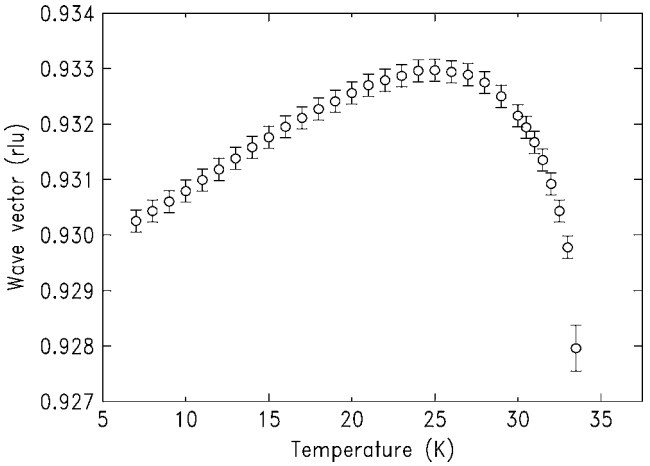

FIG. 3. Temperature dependence of the wave vector in reciprocal space measured relative to the (008) peak position using the (0 0 $8-\tau_z$) and (0 0 $8+\tau_z$) satellites measured at the Gd L_{III} edge.

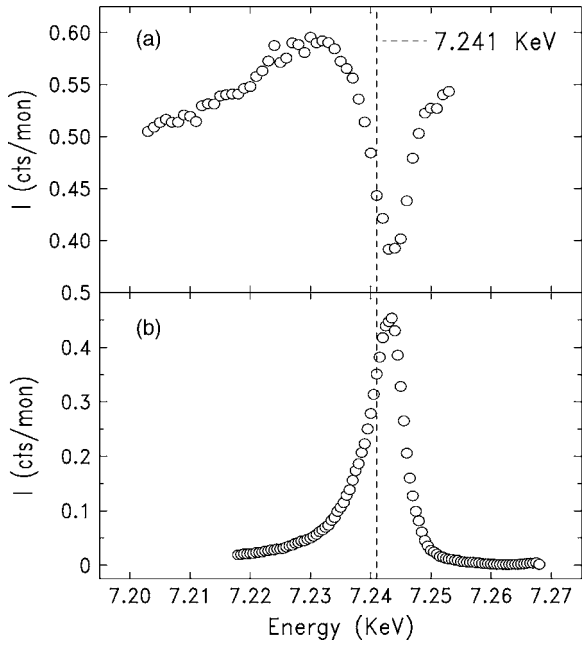

FIG. 4. Energy scans of (a) the scattered intensity at the (0 0 8) peak position and (b) the dipole resonance at the (0 0 $8-\tau_z$) satellite peak position. The dashed line marks the position of the Gd L_{III} absorption edge.

The measurement of the temperature dependence of the magnetic scattering at (0 0 $8+\tau_z$) is plotted in Fig. 5. These data were fit, close to T_N, using a power law, $I=A(T_N-T)^{2\beta}$, to determine an accurate value for T_N.[21] The intensity of the magnetic peak smoothly decreases to background levels at 33.25(±0.10)K, with $\beta=0.35(\pm 0.03)$. This value for T_N is consistent with the susceptibility measurements which show a transition at approximately 33 K.

In order to further elucidate the nature of the magnetic structure of $GdCo_2Ge_2$, a search for higher harmonics of the fundamental wave vector was performed and resulted in the observation of a very weak $3\tau_z$ satellite. The presence of

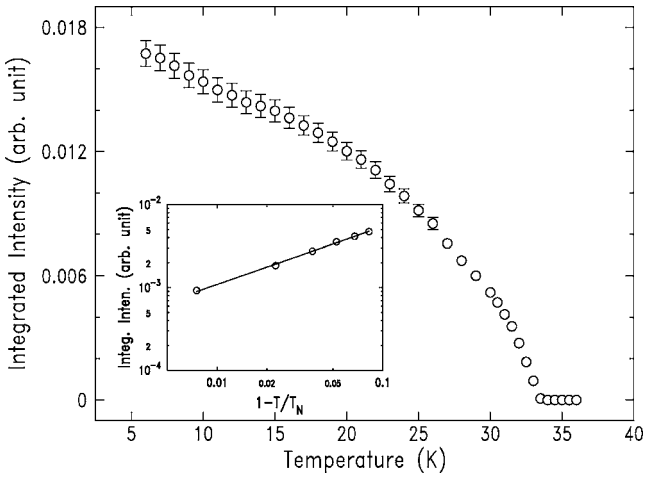

FIG. 5. Order parameter measurement used to determine T_N measured at the Gd L_{III} edge. The inset shows the plot of order parameter versus reduced temperature $(1-T/T_N)$. The solid line is a fit using a $I=A(1-T/T_N)^{2\beta}$ for temperatures close to T_N.

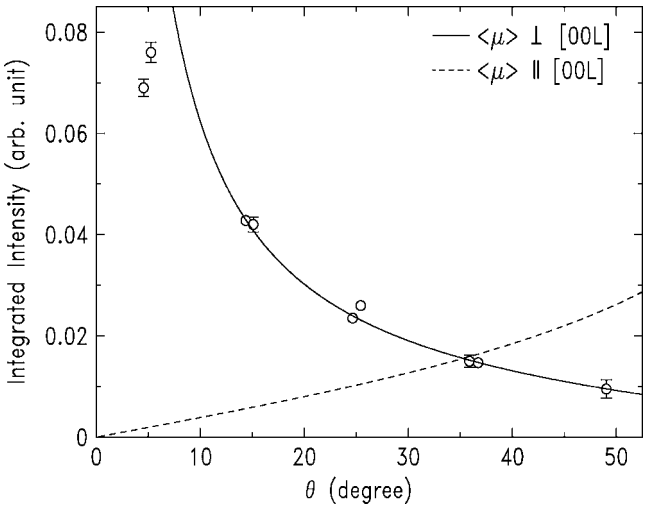

FIG. 6. Angular dependence of the integrated intensity measured at the Gd L_{III} edge at $T=6$ K. The solid line represents the theoretical prediction for a moment direction aligned perpendicular to the c axis. The dashed line represents a moment direction aligned along the c axis.

higher-order harmonics of the magnetic ordering generally indicates a squaring up of the modulation as the temperature is decreased below T_N. Alternatively, the presence of a weak third harmonic satellite is consistent with a noncollinear amplitude modulated (NCAM) structure as postulated for $GdCo_2Ge_2$ by Rotter *et al.*[1] We note that even at the lowest temperature reached in this measurement, the ratio of the intensity of the third harmonic satellite to fundamental is approximately 0.003, nearly 40 times smaller than would be expected for a fully squared structure (see Fig. 2). Indeed, above approximately 16 K the intensity of the third harmonic satellite falls below the residual charge background of our measurement. It is difficult, in these measurements, to determine whether this higher harmonic persists up to T_N or disappears at a lower temperature.

In order to determine the direction of the magnetic moment on the Gd site, the integrated intensity of the resonant scattering was measured for all magnetic satellite peaks $(0\ 0\ L\pm\tau_z)$ that could be reached in this scattering geometry. The integrated intensities were calculated from transverse scans of each peak with open detector slits to ensure proper integration. These transverse scans were fit using a Lorentzian peak profile to obtain values for the integrated intensity. The angular dependence (or Q dependence) of the integrated intensities is shown in Fig. 6 along with theoretical curves describing the dipole-resonant scattering cross sections for the magnetic moment directions along the $[00L]$ and $[H00]$ directions.

The integrated intensity in the $\sigma\rightarrow\pi$ geometry for the dipole resonant process can be written as

$$I \propto \frac{[S_L \sin(\theta) - S_H \cos(\theta)]^2}{\sin(2\theta)},$$

where $1/\sin(2\theta)$ is the Lorentz polarization factor, S_L and S_H are the components of the magnetic moment along the $[00L]$ (c axis) or $[H00]$ (a axis), respectively (for the sample orientation used in this measurement) and θ is the one-half of the scattering angle. For a moment direction along the c axis, $S_H=0$ and the resulting scattering cross-section equation is described by the dashed line in Fig. 6. For a moment direction perpendicular to the c axis (lying in the tetragonal basal plane), the scattering cross section is shown by the solid line. With the exception of the two points at low angles, the data is well-described by the solid line in Fig. 6, indicating that the ordered moments lie primarily in the basal plane of the tetragonal structure. Because of the high symmetry of the tetragonal unit cell, it is not possible to specify further the direction of the magnetic moment within the basal plane.

The discrepancy between the data and fit at low angles can be attributed primarily to the fact that the projection of the incident beam is larger than the sample at these angles. The beam cross section was $0.4(\pm0.03)$ mm $\times 1(\pm0.03)$ mm while the sample was about 3 mm $\times$ 3 mm. At $\theta\approx5$ deg, only about half of the beam is intercepted by the sample. Indeed, when this footprint correction is applied (not shown) to the two low-Q data points, the agreement with the model improves significantly. For measurements above $\theta=8$ degrees, the sample intercepted the entire beam allowing for consistent integrated intensity measurements.

An extremely useful feature of x-ray magnetic scattering is the ability to move away from the resonant scattering energy and probe the magnetic order using nonresonant magnetic scattering techniques to confirm the direction of the magnetic moment. Using the same scattering geometry, the nonresonant scattering measurement was carried out at an energy of 7 keV. This is $\sim$250 eV below the resonant energy which ensures that the resonant scattering does not contribute significantly to the integrated intensity. By moving from the PG(006) analyzer reflection to the PG(002) reflection, both the σ and π components of the scattered beam were passed by the analyzer. While this decreases the ratio of the intensity of magnetic peaks to the charge background, it allows all components of the magnetic moment to contribute to the scattered intensity at the magnetic satellite peak. In contrast to the resonant scattering measurements, this configuration is particularly sensitive to the component of the moment directed out of the scattering plane. Thus, by comparison with resonant results, the contribution of all moment directions can be determined without realignment of the sample. The results of these measurements are plotted in Fig. 7 along with the relevant calculated cross sections for nonresonant scattering.[17] As seen in Fig. 7, the nonresonant measurement confirms that the moments lie primarily in the basal plane of the tetragonal unit cell.

In order to complete our investigation of magnetic ordering in $GdCo_2Ge_2$ an attempt was made to find a measurable resonant enhancement of the magnetic satellite at the Co K edge. Although resonant enhancements at the K edges of transition metals have been observed in several instances,[18] they are generally much weaker than that typically observed at the L edges of rare earths. Nevertheless, the observation of any enhancement of the magnetic satellites at the Co K edge would provide evidence for the existence of a moment on the Co sites in this compound. Scans of the energy dependence of the magnetic scattering through the Co K edge, however,

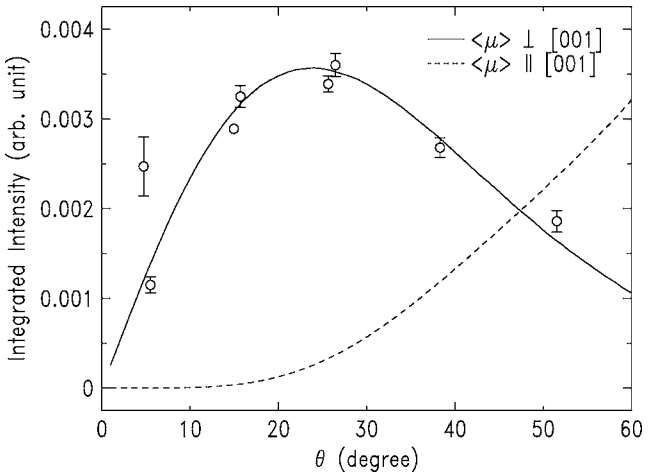

FIG. 7. Nonresonant Q dependence of the integrated intensity measured using an incident beam energy of 7 keV at $T=6$ K. The solid line represents the scattering cross section for the magnetic moment aligned perpendicular to the c axis. The dashed line represents the scattering cross section for the magnetic moment aligned parallel to c.

failed to reveal any enhancement of the magnetic peak leading us to conclude that Co does not carry a measurable moment in the magnetically ordered state of $GdCo_2Ge_2$.

IV. DISCUSSION

Through a magnetic x-ray scattering investigation of $GdCo_2Ge_2$, we have found that this compound orders in an incommensurate antiferromagnetic structure below $T_N = 33.25(\pm 0.10)$K. The modulation wave vector characterizing the oscillatory magnetic order is temperature dependent with a value of $(0\ 0\ \tau_z)$ where $\tau_z = 0.930$ rlu at the lowest temperature (6 K) of this measurement. The formation of magnetically ordered structures in the RCo_2Ge_2 compounds, characterized by a wavevector with the same symmetry as found in the isostructural RNi_2Ge_2 family of compounds, suggests that a Fermi-surface nesting mechanism is operative in the Co germanides as well.

Both the resonant and nonresonant scattering measurements confirm that the Gd moment lies primarily in the basal plane of the tetragonal unit cell. We found that the incommensurate magnetic structure persists down to the base temperature of our measurement in marked contrast to the results of previous investigations on other RCo_2Ge_2 compounds (R=Ho, Dy, Tb). While our measurements conclude that the Gd moment lies primarily in the basal plane, it is not possible to specify whether the moments are arranged in a collinear or cycloidal pattern. Nevertheless, this does imply some degree of anisotropy in the exchange coupling or a weak crystal-field anisotropy.[19,20] Finally, we note that questions regarding the temperature dependence of the magnetic wave vector and the third harmonic satellite, as well as any possible relationship between them, remain open and should be addressed by further investigations.

In comparison with other the members of the RCo_2Ge_2 family, $GdCo_2Ge_2$ does not exhibit a second transition below T_N to a commensurate antiferromagnetic structure for temperatures above 6 K. We speculate that the absence of strong CEF effects for Gd ($L=0$) depresses this transition with respect to the Ho-, Dy-, and Tb-based members. However, since CEF effects are absent for Gd, as the order parameter saturates at low temperature the magnetic order must evolve to an equal moment structure. Several possibilities exist for the $T=0$ K antiferromagnetic structure including commensurate antiferromagnetic order, a fully squared incommensurate structure or an equal moment cycloidal structure. The existence of a third harmonic magnetic satellite, albeit weak, is a particularly interesting feature of these measurements. It implies either a collinear structure that is squaring up or a weakly asymmetric (elliptical rather than circular) cycloid. If the latter is true, $GdCo_2Ge_2$ is likely the first example of a noncollinear amplitude modulated (NCAM) structure as postulated for $GdCo_2Ge_2$ by Rotter *et al.*[1]

ACKNOWLEDGMENTS

The authors would like to thank A. Kreyssig for useful discussions. Ames Laboratory is operated by Iowa State University under Contract No. W-7405-Eng-82. The Midwest Universities Collaborative Access Team (MUCAT) sector at the Advanced Photon Source is operated by the Ames Laboratory and supported by the U.S. DOE Office of Science, Basic Energy Science through Contract No. W-7405-Eng-82. The APS is operated by Argonne National Laboratory and supported by the DOE Office of Science, Basic Energy Science under contract number W-31-109-Eng-38.

*Email address: goldman@ameslab.gov

[1] M. Rotter, M. Loewenhaupt, M. Doerr, A. Lindbaum, and H. Michor, Phys. Rev. B **64**, 014402 (2001).
[2] W. M. McCall, K. S. V. L. Narasimhan, and R. A. Butera, J. Appl. Crystallogr. **6**, 301 (1973).
[3] P. Schobinger-Papamantellos, J. Rodriguez-Carvajal, and K. H. J. Buschow, J. Alloys Compd. **274**, 83 (1998).
[4] B. Penc, M. Hofmann, J. Leciejewicz, and A. Szytula, J. Phys.: Condens. Matter **11**, 7579 (1999).
[5] P. Schobinger-Papamantellos, K. H. J. Buschow, C. Ritter, and L. Keller, J. Magn. Magn. Mater. **264**, 130 (2003).
[6] H. Pinto, M. Melamud, M. Kuznietz, and H. Shaked, Phys. Rev. B **31**, 508 (1985).
[7] Z. Islam, C. Detlefs, C. Song, A. I. Goldman, V. Antropov, B. N. Harmon, S. L. Budko, T. Wiener, P. C. Canfield, D. Wermeille, and K. D. Finkelstein, Phys. Rev. Lett. **83**, 2817 (1999).
[8] Z. Islam, Ph.D. thesis, Iowa State University 1999.
[9] J. Park, D. P. Brammeier, C. G. Olson, P. C. Canfield, and D. W. Lynch, Phys. Rev. B **70**, 075105 (2004).
[10] A. Szytula and J. Leciejewicz, *Handbook of Crystal Structures*

and Magnetic Properties of Rare Earth Intermetallics (CRC Press, Boca Raton, 1994), pp. 114–192.

[11] D. Gignoux and D. Schmitt, *Handbook of Crystal Structures and Magnetic Materials* (Elsevier Science B.V., New York, 1997), Vol. 10, pp. 239–413.

[12] J. P. Hill and D. F. McMorrow, Acta Crystallogr., Sect. A: Found. Crystallogr. **52**, 236 (1996).

[13] C. Detlefs, A. H. M. Islam, A. I. Goldman, C. Stassis, P. C. Canfield, J. P. Hill, and D. Gibbs, Phys. Rev. B **55**, R680 (1997).

[14] P. C. Canfield and Z. Fisk, Philos. Mag. B **56**, 7843 (1992).

[15] P. C. Canfield and I. R. Fisher, J. Cryst. Growth **225**, 155 (2001).

[16] J. C. Lang, G. Srajer, J. Wang, and P. L. Lee, Rev. Sci. Instrum. **70**, 4457 (1999).

[17] C. Detlefs, A. I. Goldman, C. Stassis, P. C. Canfield, B. K. Cho, J. P. Hill, and D. Gibbs, Phys. Rev. B **53**, 6355 (1996).

[18] J. P. Hill, C.-C. Kao, and D. F. McMorrow, Phys. Rev. B **55**, R8662 (1997).

[19] M. Bouvier, P. Lethuillier, and D. Schmitt, Phys. Rev. B **43**, 13137 (1991).

[20] J. A. Blanco, D. Gignoux, and D. Schmitt, Phys. Rev. B **43**, 13145 (1991).

[21] Resonant scattering at the L edges of rare earths involves transitions from the $2p$ core states to the unoccupied $5d$ states. The magnitude of the resonant scattering is largely determined by the matrix element of the transitions which, in turn, depends upon the size of the exchange interaction between the $4f$ and $5d$ electrons. Therefore, at least for Gd where the $4f$-$5d$ exhange interaction is large, the resonant scattering amplitude scales with the magnitude of the $4f$ ordered moment.